Available online at www.sciencedirect.com

ScienceDirect

Advances in Space Research 55 (2015) 835–842

ADVANCES IN SPACE RESEARCH (a COSPAR publication)

www.elsevier.com/locate/asr

Properties of sunspot umbrae of leading and trailing polarity in 1917–2013

Andrey Georgievich Tlatov [a,*], K.A. Tlatova [a], V.V. Vasil'eva [a], A.A. Pevtsov [b], K. Mursula [c]

[a] Kislovodsk Mountain Astronomical Station of Pulkovo Observatory, Gagarina Str. 100, Kislovodsk 357700, Russia
[b] National Solar Observatory, Sunspot, NM 88349, USA
[c] ReSoLVE Centre of Excellence, Department of Physics, FIN-90014, University of Oulu, Finland

Received 1 February 2014; received in revised form 27 May 2014; accepted 28 May 2014
Available online 12 June 2014

Abstract

Using the software developed by us, we produced a digitized (tabulated) database of sunspot umbrae and pores observed at Mount Wilson Observatory (MWO) in 1917–2013. The database includes the heliographic coordinates, areas and the polarity and strength of magnetic fields of umbrae and pores in the MWO sunspot drawings. Using this database we study here the properties and long-term variation of sunspot umbrae and pores, separately for leading and trailing polarity spots. We find that the leading sunspots have tendency for larger umbrae and stronger magnetic field strength than the trailing spots. The average field strength and area of sunspot umbrae vary with sunspot cycle. Furthermore, the mean magnetic field strength in sunspot umbrae exhibits a gradual increase from early 1960s to 1990s. The nature of this increase is discussed.

Keywords: Solar cycle; Sunspot; Magnetic field

1. Introduction

The magnetic field is the main characteristic of sunspots, and as the magnetic field changes in time, the intrinsic properties of sunspots may also change. Synoptic measurements of sunspot magnetic fields using the Zeeman effect began in the early 20th century, and have continued until the present time. Studying the long-term variation of the magnetic fields of sunspots can provide unique information about the nature of the solar dynamo and the solar cycle. The longest series of observations of sunspot magnetic fields exists at Mount Wilson Observatory (MWO) from 1917 until the present. (Due to funding shortage, the daily sunspot measurements were stopped on 16 September 2004, but restarted on January 25, 2007). These are the very same observations based on which the fundamental laws of the solar magnetic cycle were originally established. For example, these observations were used to demonstrate that sunspots are regions of strong magnetic fields, that they often appear in the form of a bipolar magnetic field structure (Hale, 1908), and that the magnetic polarity of these bipoles changes for every 11-year sunspot cycle (Hale et al., 1919). It is now known that the magnetic fields have both cyclical and long-term variations. Several recent studies of sunspot field strengths speculate on a possible decline in their average field strength over the declining phase of cycle 23 (e.g., Livingston et al., 2012, and references therein), while some other question the origin of such a decline (e.g., Pevtsov et al., 2011, 2014). The long-term measurements such as those made at MWO allow to glean into a history of long-term changes in sunspot properties

* Corresponding author. Tel.: +7 9282522125; fax: +7 8793731088.
E-mail addresses: tlatov@mail.ru (A.G. Tlatov), ksuha-sun@list.ru (K. A. Tlatova), ksuha-sun@list.ru (V.V. Vasil'eva), apevtsov@nso.edu (A.A. Pevtsov), kalevi.mursula@oulu.fi (K. Mursula).

http://dx.doi.org/10.1016/j.asr.2014.05.033
0273-1177/

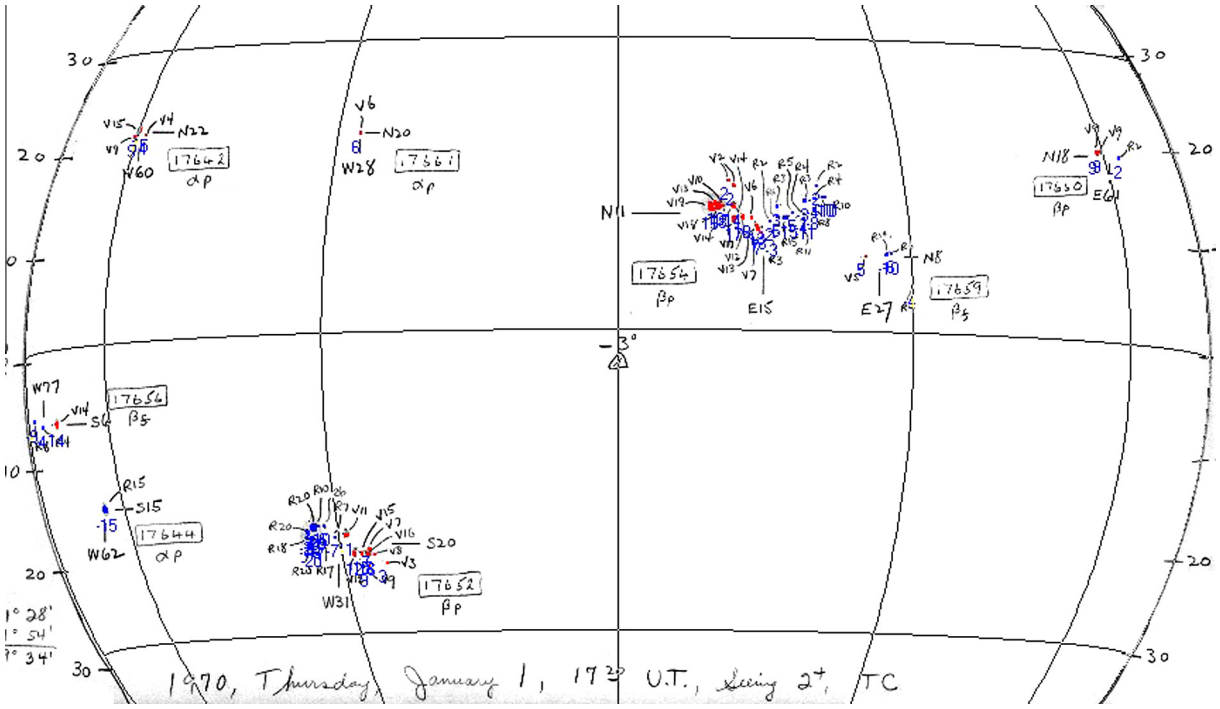

Fig. 1. A sample daily drawing of sunspots measured at MWO on January 1, 1970. On the drawing West is at the left. Sunspot umbrae are semi-automatically selected and colored according to their polarity (blue for positive and red for negative). Sunspot group numbers and coordinates, as well as the magnetic fields of umbrae are denoted in the drawing. (For interpretation of the references to colour in this figure legend, the reader is referred to the web version of this article.)

and to investigate how unique (or typical) the current solar activity is.

Pevtsov et al. (2011) studied the magnetic field strengths taken in Fe I 630.15-630.25 nm line in 1957–2010 at seven stations of the solar observatory network covering eleven time zones in the former USSR. In order to mitigate the differences in atmospheric seeing and in the level of observer experience, they included only the strongest magnetic field observations for each day. Sunspot field strengths were found to vary strongly with the solar cycle, while no definite long-term decline was noted over this time.

Pevtsov et al. (2014) digitized and studied the MWO summary tables published in the Publications of the Astronomical Society of the Pacific (PASP). These data were also made publicly available to the research community at http://www.nso.edu/node/310 for period of 1920–1958. However, these summary tables only give information on the maximum field strength measured in each active region, their mean latitude, and the date of the central meridian crossing. More detailed data are available in MWO hand-drawings only. A sample of such a map (a hand-drawing) is presented in Fig. 1. Software to digitize these MWO drawings has recently been developed (see Tlatova et al., 2013, for a discussion), and is applied to the existing digital images of drawings. This effort produced a database of solar features including the magnetic fields, areas and positions of the nuclei (umbrae of sunspots and pores) as observed at MWO in 1917–2013. In this paper, we analyze this database.

2. Data and processing method

The daily observations at Mount Wilson Observatory are carried out at the 150-foot (45.7 m) Solar Tower (http://obs.astro.ucla.edu/150_tele.html). Solar images are constructed using a coelostat and a lens, and have a diameter of about 42 cm. When taking a measurement, the observer marks the boundary of the solar disk, and draws the position and configuration of sunspots. Magnetic field measurements are then carried out by measuring the splitting of the Zeeman components. The intensity of the magnetic field at the center of the sunspot was measured visually using the iron line λ 617.3 nm in 1917–1961, and thereafter using the λ 525.0 nm line. The spot whose field is to be measured is placed at the spectrograph entrance slit, and the observer judges its polarity and magnetic field strength using micrometer with the tipping plate placed at the focal plane of the 75-foot (22.9 m) spectrograph. With this setup, sunspot polarities and field strengths can be obtained at the accuracy of a few hundred Gauss. The measured value of the magnetic field is then denoted on the drawing of the respective sunspot umbra. As a rule, all spots, umbrae and pores visible on the Sun during the day are drawn. However, in some days the field strengths were measured in only few (not all) sunspots (see, Pevtsov et al., 2014, for selected examples). Sketches of umbrae, penumbra and other magnetic structures used pencils of varying hardness that distinguished these structures by brightness. The archive of these drawings begins

in 1917, and the number of daily drawings is currently about 25,000. A majority of these drawings has been digitized (scanned), and their images are available online (ftp://howard.astro.ucla.edu/pub/obs/drawings). Fig. 2 shows annual number of drawings included in our database. In a typical year, there are about 330 clear days at MWO (R. Ulrich, private communication). Years with low number of drawings in Fig. 2 are when the observations were taken, but not all drawings were scanned to a digital format. Due to the program shutdown, the total number of sunspot drawings made in 2005 and 2006 was nine and two, accordingly.

The change in the spectral line in 1962 was accompanied by a change in the tip plate. In 1978, a flooding of the spectrograph pit damaged the spectral grating, which was replaced in 1982. (Prior to that, five different gratings were used between 1932 and 1978). The grating was replaced again in mid-1990. The reader can find a more detailed discussion of the instrumental changes in Livingston et al. (2006).

The digitization of the MWO scanned drawings is done in the following steps. In the first step the code identifies and fits the solar limbs to the image. This establishes the transformation between the image and the heliographic coordinates. Next, the operator manually selects the location of individual umbrae and pores to be digitized. The program automatically detects their outer boundaries following the procedure described in Tlatov et al. (2014). Then, the operator manually enters the intensity and polarity of the magnetic field of the respective structure. At each step, the operator verifies the validity of the automatic selection and can make adjustments to the automatic action when necessary.

For each selected umbra and pore, we measured and stored its heliographic coordinates, the number of pixels covered, the area corrected for the heliographic projection, the time of observations, and the strength and polarity of its magnetic field. We analyzed all observation days that are presently available as digital (scanned) images and during which magnetic field measurements were made. There are about 16,000 such daily drawings. The total number of magnetic field measurements of individual umbrae and pores is 336,459. Unfortunately, not all drawings are yet digitized (scanned). We plan to include additional data to our database, when more drawings are converted to digital images.

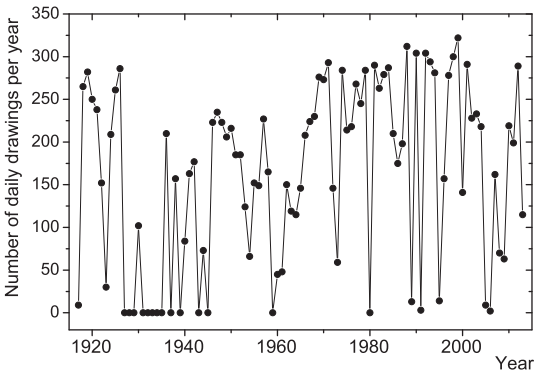

Fig. 2. Annual number of digitized drawings included in our database.

Until October 1961, the numbers recorded on drawings corresponded to the angle of tip plate. However, the design of the micrometer provided an approximate scaling of about 1 degree tip angle corresponding to 100 G field strength. The relation between the displacement and the tip angle is non-linear, and the non-linearity increases for larger tip angles (stronger field strengths). In October 1961, the tip plate was replaced by a thicker one, which increased the non-linearity for stronger fields. From 1961 to 1994, the number recorded on drawings corresponded to the tip angle divided by 2, which approximately corresponds to field strength in 100 G up to 1600 G field. Larger fields are significantly underestimated. From 1994, the observer records actual field strength derived from a look-up table. These non-linearities were corrected following to Livingston et al. (2006) recipe.

3. Systematic trends in the data set

Fig. 3 shows the time evolution of several parameters derived from the sunspot data set. There are large gaps in the data, especially in the 1930s and 1940s, and solar cycle 16 is covered particularly sporadically. In spite of that, the data exhibit several clear trends. Thus, for example for the average area and the average strength of the magnetic field, there is a disparity between the early part

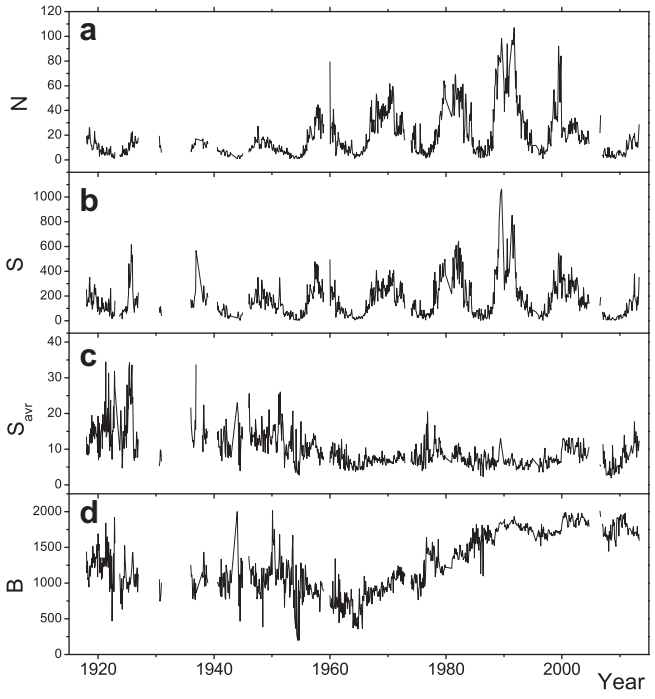

Fig. 3. Monthly means of (a) the number of measured umbrae and pores per daily drawing, (b) the total area of all measured umbrae and pores in a drawing in units of μhm, (c) the average area of measured umbrae and pores in units of μhm, (d) the average strength of the magnetic field of the measured umbrae and pores in units of Gauss.

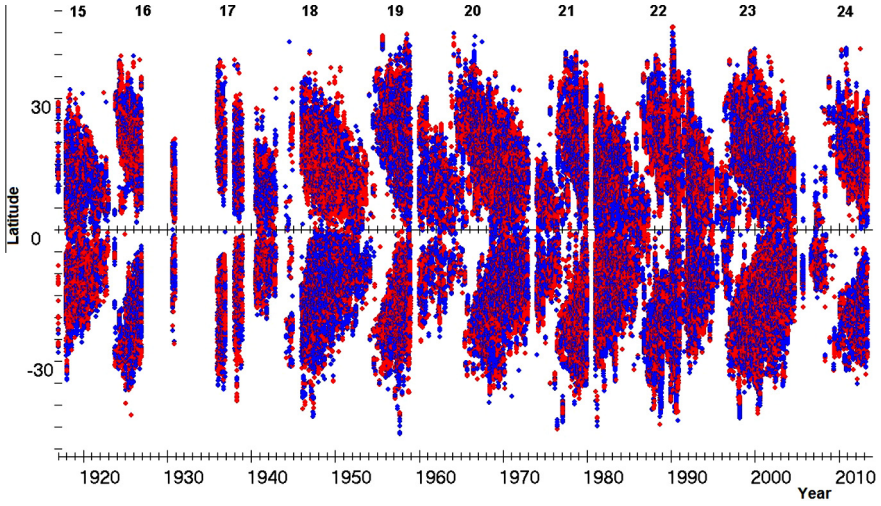

Fig. 4. The latitude-time diagram of the measured umbrae and pores with magnetic field polarity indicated in color (blue for positive and red for negative polarity). Above presented the number of activity cycles. (For interpretation of the references to colour in this figure legend, the reader is referred to the web version of this article.)

(1917- roughly 1961) and the later part (1962–2013) of the data set. The average number of magnetic field measurements per daily drawing is significantly lower during the early part of the data set as compared with the later period. The amplitude of solar cycle variations is also significantly lower in 1917–1961 (see Fig. 3(a)). A similar trend can be seeing in the total area of measured solar features (sunspot umbrae and pores, Fig. 3(b)). Therefore, the difference in solar cycle amplitudes cannot be attributed to the variations in strength of solar activity during these periods. According to the international sunspot number, solar cycles 18–19 were higher than any cycles of 1961–2013 period. One would expect that these high cycles would produce a larger number of umbrae and pores, but Fig. 3(a) does not fit that expectation. Average area of all measured features on each drawing (Fig. 3(c)) suggests a different trend: it is systematically larger in 1917–1961 than in 1962–2013. Taken together, Fig. 3(b) and 3(c) imply that during the early period in 1917–1961, the MWO drawings record a smaller number of features, but on an average the features have larger areas. During the later period in 1962–2013, the drawings contain larger number of smaller features. This change in the number of features for which the magnetic field was measured can be attributed to instrumental changes. For example, using the Fe I 525.0 nm spectra line with a significantly higher Lande factor $g = 3.0$ would allow the observers to measure weaker fields after 1961, which they could not reliably measure with Fe I I 617.3 nm Lande factor $g = 2.5$ spectral line used earlier. The visual inspection of drawings also suggests a higher "granularity" in observations in 1960–2013 (e.g., more instances when the field is measured in separate umbrae within complex sunspots). This change was noted earlier in Pevtsov et al. (2014), who attributed it to the observer "learning curve" effect.

Finally, the average field strength (Fig. 3(d)) shows a strong increasing trend from early 1960s till late-1980s. The change is gradual, which argues against a pure instrumental effect (which should result in a more abrupt change). Still, we believe that the change in instrumentation does play a role. Visually, we see that the drawings taken after early 1960th show much more details, which suggests other changes in instrumentation (e.g., reduction in scatter light, or width of spectrograph slit). Changing the spectral line to the one with large Lande factor also enabled observers to measure much weaker fields. This could lead to the observer taking more measurements inside single sunspots (but with multiple) umbrae ("learning curve" as suggested by Pevtsov et al., 2014). Since the data only show changes in a mean field strength, but not in area of sunspots, we argue that this trend is not solar in its origin. Further investigation of these aspects is currently underway in a separate study.

Fig. 4 depicts the butterfly diagram (latitude-time plot) of the measured umbrae and pores. Each umbra and pore are marked at its position, and colored with its magnetic polarity, using blue for positive and red for negative polarity. Note that each wing of the butterfly is dominated by the color of the leading polarity umbrae due to the larger number of leading polarity umbrae (see later). For example, the northern wing of solar cycle 22 is dominated by red color, which corresponds to a negative polarity field. Note also that, despite the considerably smaller number of measured umbrae from 1917 until 1950, their latitudinal range is not significantly smaller than during the later time intervals with more complete daily coverage. Thus, despite a courser daily coverage for example in 1930–1940, our data set is still representative of the whole sunspot family.

4. Areas of umbrae of leading and trailing polarity

Whatever the nature of the systematic trends in the data set described in previous section, we expect them to affect equally the sunspots of leading and trailing polarity, and

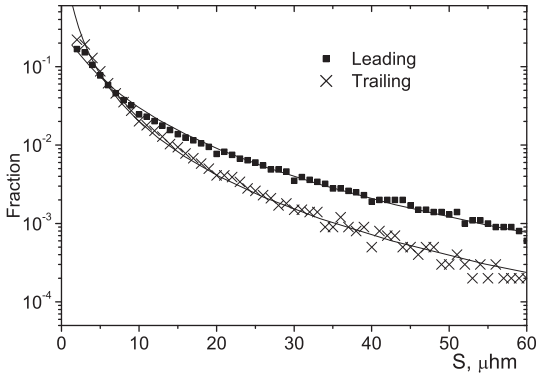

Fig. 5. Normalized distribution of measured umbral area (in millionth of solar hemisphere, μhm) for leading and trailing polarity umbrae and pores.

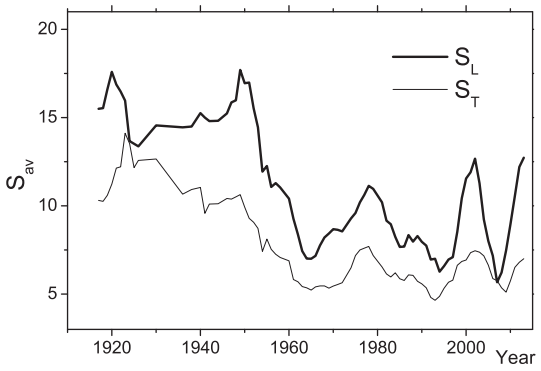

Fig. 6. The 5-year running mean areas of umbrae and pores of leading (SL) and trailing (ST) polarity in units of μhm.

therefore, the above-mentioned trends should have no effect on the comparative properties of these two groups of sunspots. In our database, there are approximately 185,800 spots of leading polarity and 150,000 spots of trailing polarity. Fig. 5 shows the distribution of sunspot umbrae by their size (area) for these two groups. The bin-size used for this plot is 1 μhm (millionth of solar hemisphere), and each histogram is normalized by the total number of spots in each group. As the measurements of sunspots near solar limb show a large scatter, we restricted the heliocentric distance of features included in this plot by $r/R < 0.7$ and $S \geqslant 2$ μhm.

It is quite clear that there is a deficit of umbrae with large size (>10 μhm) in the group of sunspots of trailing polarity. The dependence of the relative fraction f_L of the leading umbrae on area (S) can be quantified with the following second order polynomial: $\log(f_L) = (-0.57 \pm 0.08) - (0.35 \pm 0.12)\log(S) - (0.60 \pm 0.04)\ \log^2(S)$. For umbrae of trailing polarity the fit is $\log(f_T) = (0.176 \pm 0.070) - (0.38 \pm 0.10)\log(S) - (0.62 \pm 0.03)\log^2(S)$ (see Fig. 5).

The asymmetry in size between the umbrae of leading and trailing polarity is in agreement with the known properties of solar active regions. Typically, the leading polarity flux is more compact and has stronger field strength than the magnetic flux of trailing polarity. Morphologically, the leading polarity is typically concentrated in a large coherent sunspot, while the trailing polarity consists of a more dispersed smaller spots or pores (for review of these observations, see Fan et al., 1993; Fisher et al., 2000; Vitinsky et al., 1986).

The mean area of umbrae and pores exhibits long-term variations. Fig. 6 shows the time evolution of the average area separately for the leading and trailing polarity umbrae and pores. We used 5-year running means to smooth out the highly varying monthly values (see Fig. 3(c)) in order to emphasize the long-term trends. The averaged area of the leading polarity is systematically larger than the area of umbrae of the trailing polarity, in agreement with distribution in Fig. 5. Both leading and trailing polarity umbrae show a gradual decline between 1917 and early 1960s, whose nature is yet unclear. Qualitatively, this gradual decrease supports the idea that there is a "learning curve" effect in MWO data, i.e., that over the time, the drawings became progressively more detailed, which resulted in a decrease in size of individual features. Note that the time interval of the more or less constant mean area since the early 1960s approximately coincides with the start of the new observation system (see data section). We speculate that a smaller mean (area) during this period is likely due to a larger number of measured features (umbrae and pores) as compared with early period of observations (1917–1960).

5. Magnetic fields of umbrae of leading and trailing polarity

Figs. 7 and 8 show the time evolution of the monthly averaged values of magnetic field strengths for umbrae and pores of leading and trailing polarity. In both figures we have also included the mean strengths of the magnetic fields weighted by the umbral area: $B^W = \sum(B \cdot S)/\sum S$. The overall mean strength of magnetic fields of the leading umbrae (without weighting) is $B_L \approx 1700$ G and $B_L^W \approx 1820$ G with weighting. The corresponding strengths for the trailing polarity umbrae are $B_T \approx 1480$ G and $B_T^W \approx 1530$ G, respectively. Thus, the mean magnetic field strengths of the trailing umbrae are roughly 15–18% smaller than the those of the leading umbrae. This asymmetry between field strength of leading and trailing polarities is in agreement with the well-known properties of active regions as we discussed in the previous section.

Fig. 9 shows the differences in the distributions of magnetic field strength in umbrae and pores of leading and trailing polarity. The maxima of both distributions are found at about $B \sim 1700$–1800 G. However, in comparison with the trailing polarity, the leading polarity exhibits a deficit in fraction of features with weaker field strength, and an excess of features with stronger field strengths. Also Fig. 9 suggests the existence of two populations with a separation between two somewhere between 1000–1500 G. The two populations can be related to contribution from pores (weaker fields) and sunspot umbrae (stronger fields).

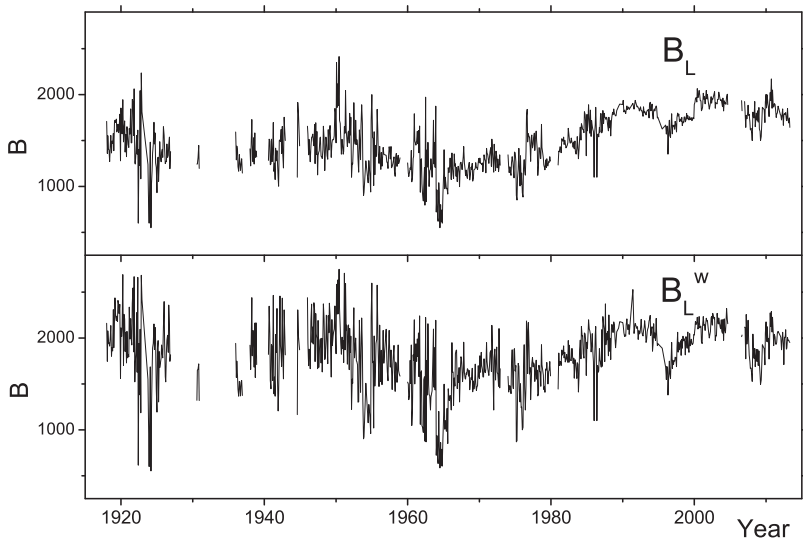

Fig. 7. Monthly mean magnetic field strengths of umbrae and pores of leading polarity. Top: non-weighted strengths; bottom: strengths weighted by area.

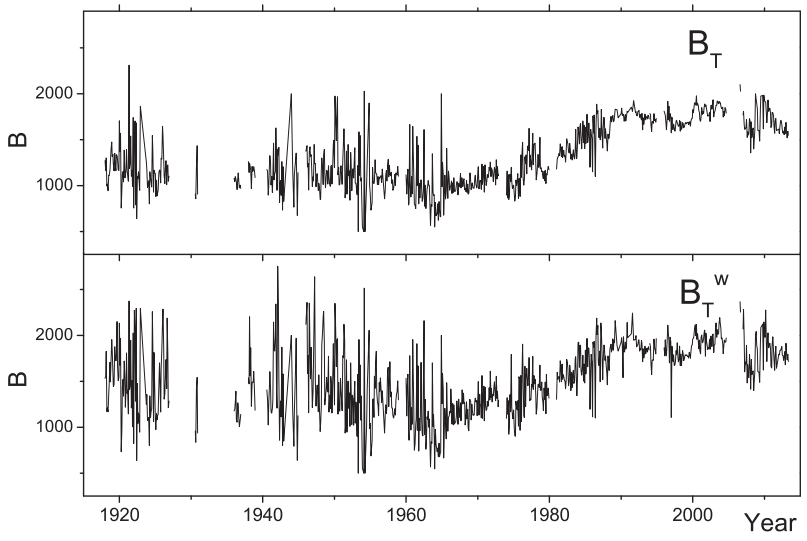

Fig. 8. Monthly mean magnetic field strengths of umbrae and pores of trailing polarity. Top: non-weighted strengths; bottom: strengths weighted by area.

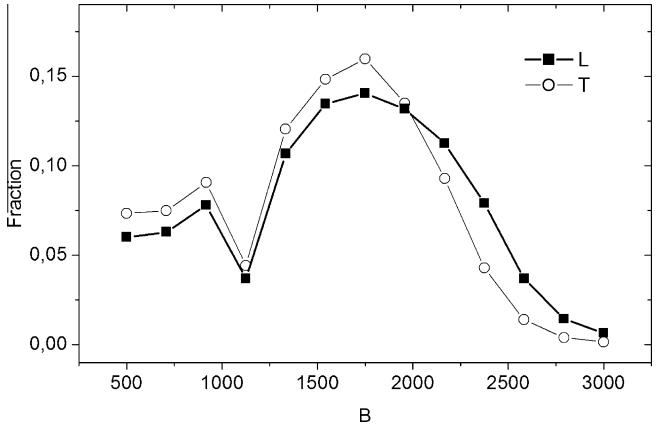

Fig. 9. Fractional histogram distribution of magnetic field strengths of umbrae and pores of leading (L) and trailing (T) polarity. Only umbrae within 70% of solar radius from the center are included.

As the measurements of sunspots near solar limb show a large scatter, we restricted the heliocentric distance of features included in this plot by $r/R < 0.7$. We believe that the scatter in the field strength measurements for features close to the limb could be the result of several things, including (1) strong foreshortening of features, making it more difficult for the observer to select an area with the strongest field and (2) increasing effects of a (both polarized and non-polarized) scattered light in a near limb feature. While the observing method allows to measure the full field strength, scattering from penumbra and even surrounding photosphere may inhibit the correct measurement of field strength in a near limb feature. However, even with this limitation, Fig. 9 is representative of the entire data set as only about 29% of the data set are excluded from this figure.

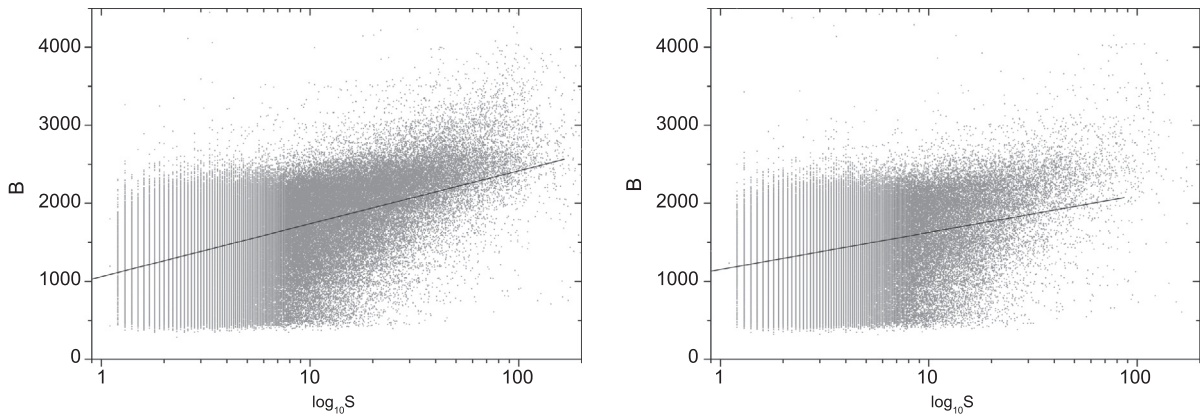

Fig. 10. Scatter plot of magnetic field strength and the logarithm of the area of sunspot umbrae and pores for the leading (left) and trailing (right) spots. Best fit line is included.

6. Sunspot area as proxy for magnetic field strength for leading and trailing sunspots

Using earlier MWO data, Ringnes and Jensen (1960) found a strong correlation between the logarithm of sunspot area and its field strength. The presence of such correlation was later confirmed by several authors, including recent observations from the Helioseismic and Magnetic Imager (HMI) on board the Solar Dynamics Observatory (SDO). Here, we study this relationship separately for sunspots of the leading and trailing polarity (Fig. 10). Despite significant scatter, the data show a clear tendency for a correlation between the umbral areas and the maximum field strength. The dependency is looser than compared with modern measurements from space (Tlatov and Pevtsov, 2014); the scatter can originate from the atmospheric seeing conditions affecting both area and the field strength measurements and by the fact that the steepness of the linear dependency varies with solar cycle (see below). The measurement error of a few hundred Gauss and the uncertainties in areas derived from hand drawings may also contribute to the scatter in Fig. 10. In respect to errors in the field strength, one can argue that the method is limited to the Zeeman splitting exceeding the Doppler width of the spectral lines. According to this argument, a typical Doppler width of Fe I 617.3 nm makes field strength measurements <1000 G unreliable. Still, as was noted by Livingston et al. (2006), a trained observer can consistently measure weak magnetic field below 1000 G. Thus, we took a conservative approach and restricted Fig. 10 to magnetic fields stronger than 500 G.

We find the following linear best fit for the leading umbrae: $B_L = 1057 + 679 \cdot \log(S)$ (correlation coefficient $r = 0.5$), and for trailing umbrae: $B_T = 1151 + 476 \cdot \log(S)$ ($r = 0.3$). In fact, we note that the relation depicted in Fig. 10 is somewhat nonlinear, and the following best fit second order polynomial can be found for the leading spots: $B_L = 1301 - 9.9 \cdot \log(S) + 378 \cdot \log^2(S)$, and for the trailing spots: $B_T = 1330 - 102 \cdot \log(S) + 368 \cdot \log^2(S)$. The non-linearity may partly arise from imposing a lower cutoff (500 G) for the measurement of the magnetic field strength.

Table 1 shows the coefficients a and b (and the respective correlation coefficients) of the linear fit $B = a + b \cdot \log(S)$ to the data separately for the leading and trailing umbrae for different solar cycles. The correlation coefficients calculated for the individual solar cycles are larger than one for the total set. This is due to the fact that the slope of the studied relationship varies greatly (mainly decreasing) in time, as seen in Table 1. Pevtsov et al. (2014) noted a correlation between the slope and the amplitude of the solar cycle.

Table 1
Constants for the linear relation between magnetic field strength and the logarithm of the area for leading (L) and trailing (T) umbrae.

Cycle	a_L	b_L	r_L	a_T	b_T	r_T
15	280.0 (±18.1)	1262.0 (±16.5)	0.700	439.0 (±19.9)	943.0 (±21.7)	0.56
16	475.0 (±19.5)	883.0 (± 17.3)	0.620	584.0 (±20.3)	659.0 (±20.8)	0.49
17	−4.0 (±24.9)	1294.3 (± 22.2)	0.725	146.0 (±27.7)	1054.0 (±28.0)	0.63
18	67.3 (±18.7)	1371.6 (±16.2)	0.725	295.0 (±21.1)	1023.0 (±21.7)	0.57
19	193.4 (±12.7)	1192.2 (±12.6)	0.740	351.0 (±14.5)	940.0 (±17.3)	0.61
20	466.0 (± 5.8)	1064.0 (± 7.2)	0.683	547.0 (±6.6)	851.0 (±9.9)	0.51
21	911.0 (±3.8)	744.5 (± 4.7)	0.650	942.0 (±4.4)	672.0 (±6.4)	0.53
22	1407.0 (±3.1)	666.0 (± 4.6)	0.625	1428.0 (±3.5)	580.0 (±6.0)	0.49
23	1382.9 (±2.9)	596.5 (±3.5)	0.710	1413.0 (±3.3)	522.0 (±4.8)	0.56
24	1349.8 (±7.2)	545.4 (±7.7)	0.700	1364.0 (±8.2)	474.0 (±11.4)	0.56

We also note that for each individual cycle, the correlation coefficients calculated for the leading polarity features (average $r_L \approx 0.68$) are systematically higher than for the trailing umbrae (average $r_T \approx 0.55$). The slopes b_L of the leading polarity features are about 20% larger than those of the trailing umbrae. This seems to be in line with the expectation that the leading polarity fields are stronger and more compact in comparison with the features associated with the trailing polarity fields.

7. Conclusions

We used the software developed by us to digitize (tabulate) the digitized (scanned) daily drawings from the Mount Wilson Observatory in 1917–2013. We employed the data to investigate properties of sunspot umbral areas and field strengths over the period of nine solar cycles (cycles 15–23). The data show several long-term trends, which could be of solar origin, or may be related to changes in statistical properties of the data set (e.g., increase in number of features identified on drawings by the observer). We plan a separate study to investigate this in more detail.

Separating the data into two groups associated with leading and trailing polarity fields reveals a dichotomy: umbrae and pores of leading polarity tend to be larger and have stronger field strength than the trailing polarity features. This dichotomy can be explained by the known property of solar active regions: leading polarity is more organized while trailing polarity is more dispersed. However, our results provide firm statistics in support of these known properties. No such statistics was ever presented before.

Finally, we verify the (approximately linear) relation between the magnetic field strength and the logarithm of umbral area separately for leading and trailing polarities. We find that the correlation between the area and the field strength is about 20% stronger for features (umbrae and pores) of the leading polarity as compared with the trailing polarity. The slope of linear dependency between these two parameters is steeper for features of leading polarity fields. This difference in steepness can be explained by a deficit of features with smaller areas and weaker fields in the group associated with the leading polarity fields. A larger number of data points in the part of the distribution function of smaller areas and weaker fields reduces the slope of linear fit for trailing polarity features.

Acknowledgments

The work was supported by the Russian Foundation for Basic Research (RFBR), the Russian Academy of Sciences and the Russian Federal Agency for Science and Innovations. We acknowledge the financial support by the Academy of Finland to the ReSoLVE Center of Excellence (Project No. 272157). National Solar Observatory (NSO) is operated by the Association of Universities for Research in Astronomy, AURA Inc under cooperative agreement with the National Science Foundation (NSF).

References

Fan, Y., Fisher, G.H., Deluca, E.E., 1993. The origin of morphological asymmetries in bipolar active regions. ApJ 405, 390–401.

Fisher, G.H., Fan, Y., Longcope, D.W., Linton, M.G., Pevtsov, A.A., 2000. The solar dynamo and emerging flux. Solar Phys. 119, 119–139.

Hale, G.E., 1908. On the probable existence of a magnetic field in sunspots. ApJ 28, 315–343.

Hale, G.E., Ellerman, F., Nicholson, S.B., Joy, A.H., 1919. The magnetic polarity of sun-spots. ApJ 49, 153–186.

Livingston, W., Harvey, J.W., Malanushenko, O.V., Webster, L., 2006. Sunspots with the strongest magnetic fields. Solar Phys. 239, 41–68.

Livingston, W., Penn, M.J., Svalgaard, L., 2012. Decreasing sunspot magnetic fields explain unique 10.7 cm radio flux. ApJ 757, L8–12.

Pevtsov, A.A., Nagovitsyn, Y., Tlatov, A., Rybak, A., 2011. Long-term trends in sunspot magnetic fields. ApJ 742, L36–40.

Pevtsov, A.A., Bertello, L., Tlatov, A.G., Kilcik, A., Nagovitsyn, Y.A., Cliver, E.W., 2014. Cyclic and long-term variation of sunspot magnetic fields. Solar Phys. 289, 593–602.

Ringnes, T.S., Jensen, E., 1960. On the relation between magnetic fields and areas of sunspots in the interval 1917–56. Astrophys. Norvegica 7, 99–121.

Tlatova, K.A., Vasilyeva, V.V., Tlatov, A.G., 2013. Variation of sunspot magnetic field in 1917–2013. ull. Crimean Astrophys. Obs. 109 (4), 7684.

Tlatov, A.G., Pevtsov, A.A., 2014. Bimodal distribution of magnetic fields and areas of sunspots. Solar Phys. 289, 1143–1152.

Tlatov, A.G., Vasilyeva, V.V., Makarova, V.V., Otkidychev, P.A., 2014. Applying an automatic image-processing method to synoptic observations. Solar Phys. 289, 1403–1412.

Vitinsky, Yu.I., Kopecky, M., Kuklin, G.V., 1986. The statistics of sunspots (Statistika pjatnoobrazovatelnoj dejatelnosti solntsa), Moscow: Nauka, 397 pp. (In Russian).